

SCIENTIFIC REPORTS



OPEN

Histamine causes endothelial barrier disruption via Ca^{2+} -mediated RhoA activation and tension at adherens junctions

Daniela Kugelmann , Lukas Thomas Rotkopf , Mariya Yosifova Radeva, Alexander Garcia-Ponce, Elias Walter & Jens Waschke

During inflammation, the disruption of the endothelial barrier leads to increased microvascular permeability. Whether tension along cell junctions contributes to histamine-induced endothelial barrier disruption remains unknown. Rapid Ca^{2+} influx induced by both histamine and thrombin was accompanied by endothelial barrier breakdown revealed as drop of transendothelial electric resistance in primary human microvascular endothelial cells. Interestingly, GLISA measurements revealed activation of RhoA but not inactivation of Rac1 at the time-point of barrier breakdown. FRET measurements showed activation of RhoA at intercellular junctions after both thrombin and histamine exposure. Breakdown coincided with increased stress fiber formation but not with translocation of vinculin, which was located along junctions in the resting state similar to postcapillary venules *ex vivo*. Moreover, increased tension at AJs was indicated by immunostaining with a conformation-sensitive antibody targeting the α 18-subunit of α -catenin. Ca^{2+} chelation by BAPTA-AM and ROCK1 inhibition by Y27632 abolished both increase of tension along AJs as well as barrier dysfunction. Moreover, BAPTA-AM decreased RhoA activation following histamine stimulation, indicating a key role of Ca^{2+} signaling in barrier breakdown. Taken together, in response to histamine, Ca^{2+} via RhoA/ROCK activation along endothelial adherens junctions (AJs) appears to be critical for barrier disruption and presumably correlated with enhanced tension. However, vinculin appears not to be critical in this process.

The endothelium provides a selective barrier between the blood and the surrounding interstitial tissue providing nutrients to the tissues, regulating vascular homeostasis and the transmigration of leukocytes, preserving tissues through oncotic pressure control and participating in tumor neoangiogenesis and inflammatory reactions^{1–4}. Endothelial cells are highly dynamic and are constantly subject to changes due to mechanical forces, and endothelial cell junctions together with the glycocalyx form the endothelial barrier⁵. Within the intercellular contacts, tight junctions (TJs) directly limit paracellular permeability whereas adherens junctions (AJs) mechanically couple neighboring cells⁶. Both junction types are functionally linked with the cortical actin cytoskeleton through several adaptor molecules. Therefore, intracellular signaling affecting actin dynamics is essential in regulating endothelial barrier function^{7–10}.

At the molecular level, AJs in endothelial cells are composed of vascular endothelial (VE-) cadherins, which allow for intercellular linkage with their extracellular domains in a Ca^{2+} -dependent homophilic manner¹¹. VE-cadherin is also crucial for endothelial barrier maintenance and recovery. The cytoplasmic domain of the VE-cadherin tail has binding sites for p120 catenin, which has been indicated to control VE-cadherin turnover, lateral clustering and junction integrity⁸, as well as β -catenin and γ -catenin, which, subsequently bind to α -catenin, sequentially, linking the whole complex directly and/or indirectly via adaptor molecules to the actin cytoskeleton^{12–15}. Cadherin complexes have been shown to not only transmit force but also act as active mechanosensors¹⁶. In this context, the adaptor protein vinculin, which anchors the cadherin complex via α -catenin to the actin cytoskeleton, is involved^{17–20}. Vinculin interaction with AJ proteins protects VE-cadherin junctions from opening during their force-dependent remodeling^{16,21}. One of the most potent signaling pathways for stabilization of the barrier properties is regulation of actin dynamics through cyclic adenosine monophosphate (cAMP)⁷.

Institute of Anatomy and Cell Biology Department I, Ludwig-Maximilians-Universität München, Munich, Germany. Correspondence and requests for materials should be addressed to J.W. (email: jens.waschke@med.uni-muenchen.de)

Furthermore, small GTPase family members, especially Rac1, Cdc24 and RhoA are crucial for regulation of the endothelial barrier^{3,5,7,22}. Therefore, a fine balance between the activities of RhoA and Rac1 GTPases is required to maintain AJs²³. Interestingly, we demonstrated in a former study that cAMP stabilizes the endothelial barrier via Rac1. Rac1 activation stabilizes the endothelial barrier against vasoactive stimuli *in vitro* and *in vivo*^{24,25}, whereas RhoA has a diverse function in endothelial barrier regulation^{5,26}.

RhoA effectively modulates the organization and dynamics of the actin cytoskeleton¹¹. Furthermore, RhoA was found to induce the disassembly of endothelial AJs in response to inflammatory conditions²³. Vasoactive mediators such as lipopolysaccharide (LPS) or tumor necrosis factor alpha (TNF- α) inhibit cAMP/Rac1 signaling and cause strong activation of RhoA⁵. RhoA activation leads to breakdown of the barrier, which is accompanied by the formation of gaps and stress fibers. This breakdown is caused by opening of interendothelial junctions in post-capillary venules which results in severe subcutaneous and whole-body cavity edema³. Although considerable research interest in the mechanisms underlying barrier disruption is evident, the significance of tension generation during acute barrier breakdown is still unclear. In this study, we used the inflammatory mediator histamine, which has been shown to regulate endothelial properties through activation of the type I histamine receptor and Rho A signaling^{27,28}, to study the mechanisms involved in anaphylaxis in primary human microvascular endothelial cells *in vitro*, and microvascular rat mesentery vessels *in vivo*. Here, we propose that histamine-mediated disruption of endothelial barrier function is Ca²⁺- and Rho kinase-dependent and correlates with enhanced tension at AJs.

Results

Histamine and thrombin induce AJ disruption and barrier dysfunction. Barrier function in endothelial cells is controlled by AJs and TJs, which are disrupted during pathological states²⁹. To elucidate the time course under which endothelial monolayers react to the short-term vasoactive mediators, histamine and thrombin, immunofluorescence analysis of vascular endothelial cadherin (VE-cadherin), filamentous actin (F-actin), and vinculin was performed at several time points. After the addition of either histamine for 3, 10 and 60 min or thrombin for 5 min, confluent HDMEC monolayers were fixed and stained for VE-cadherin (Fig. 1A) and labeled for F-actin using Alexa 488 phalloidin (Fig. 1B). Consistent with reports in the literature²⁷, short-term incubation with thrombin and histamine led to intercellular gaps- and increased stress fiber formation. Three minutes after histamine addition, intercellular gaps formed (Fig. 1A, arrows) and increased stress fiber formation was detected (Fig. 1B). Thrombin led to similar but stronger effects after 5 min of incubation. Ten minutes after histamine incubation, the intercellular gaps had largely closed. After 60 min of incubation, stress fiber formation was barely visible, and the intercellular gaps were no longer detectable (Fig. 1A–C). In contrast to control conditions, during the initial response, the linear formation of VE-cadherin at the intercellular membrane was disrupted and VE-cadherin distribution appeared a ragged (Fig. 1A). Furthermore, staining of vinculin and VE-cadherin in HDMECs under control conditions or after 3 min of histamine incubation (Fig. 1D–F) showed that vinculin staining was detectable on the cell membrane under both control and inflammatory conditions and that vinculin largely co-localized with VE-cadherin (Supplementary Fig. S1A).

In parallel, endothelial breakdown was detected by transendothelial electric resistance (TER) measurements. For that purpose, HDMECs were grown to confluence and then incubated with histamine or thrombin. Histamine induced subtle and transient barrier dysfunction and basal resistance was significantly reduced to $93.5\% \pm 0.8\%$ after 0.5 min. Recovery to baseline was evident after 3.5 min. Then, TER continued to rise above control values, which were stable for the 60 min incubation period. In contrast, thrombin induced a stronger drop in TER ($78.6\% \pm 3.7\%$), which recovered more slowly. In addition, specific inhibitors of histamine receptor type I, diphenhydramine (DPH) and histamine receptor type II, ranitidine (RAN) were preincubated with HDMECs for 15 min before the addition of histamine. As expected, diphenhydramine blocked the initial resistance drop whereas ranitidine had no significant effect (Fig. 1G,H).

Increased α 18-catenin staining indicates higher tension along AJs during the initial histamine response.

A conformation-sensitive antibody targeting the α 18-subunit of α -catenin (α 18-catenin) was used. It has been described that antibody binding correlates with tension at AJ because the epitope it binds to, is exposed during tension³⁰. Morphologically, stronger but discontinuous staining of α 18-catenin primarily along cell borders was detectable after 3 min of histamine incubation compared to control (Fig. 2A). Staining of vinculin at the cell border was observed under control conditions and colocalization with α 18-catenin did not differ significantly after addition of histamine (Fig. 2B, Supplementary Fig. S1B). Quantifications of the relative fluorescence intensity revealed that the mean changes in α 18-catenin-staining after histamine addition were $201.1\% \pm 10.0\%$, $152.9\% \pm 15.6\%$ and $114.3\% \pm 22.4\%$ of control, after 3, 10 and 60 min, respectively, whereas thrombin increased α 18-catenin-staining by $189.7\% \pm 9.2\%$ at the border (Fig. 2D) but not in the cytoplasm (Fig. 2E). In contrast, the fluorescence intensity of vinculin did not significantly change at the cell borders or cytoplasm (Fig. 2D,E). In addition, histamine transiently induced a dotted staining pattern resembling focal adhesions which was reflected in a not significant increase of vinculin staining intensity in the cytoplasm and which was also detectable following treatment with thrombin.

Activation of Rho GTPases and Ca²⁺ influx under inflammatory conditions.

The ability of endothelial cells to contract involves myosin light chain phosphorylation via myosin light chain kinase (MLCK) and Rho family proteins³¹. Of these, RhoA and Rac1 have been reported to play major roles in the short-term inflammation response^{26,27,32}. Intracellular GTP-bound Rac1 or RhoA levels were measured by GLISA after the addition of either thrombin or histamine following a standard protocol. GLISA measurements revealed significant activation of RhoA to $232.4\% \pm 17.9\%$ of control after incubation with histamine for 3 min (Fig. 3A) and $421.8\% \pm 33.4\%$ after 5 min of thrombin treatment (Fig. 3B). There were no significant changes after either incubation of histamine for 10 min or 60 min as well as thrombin for 60 min (Fig. 3A,B). Under the same conditions,

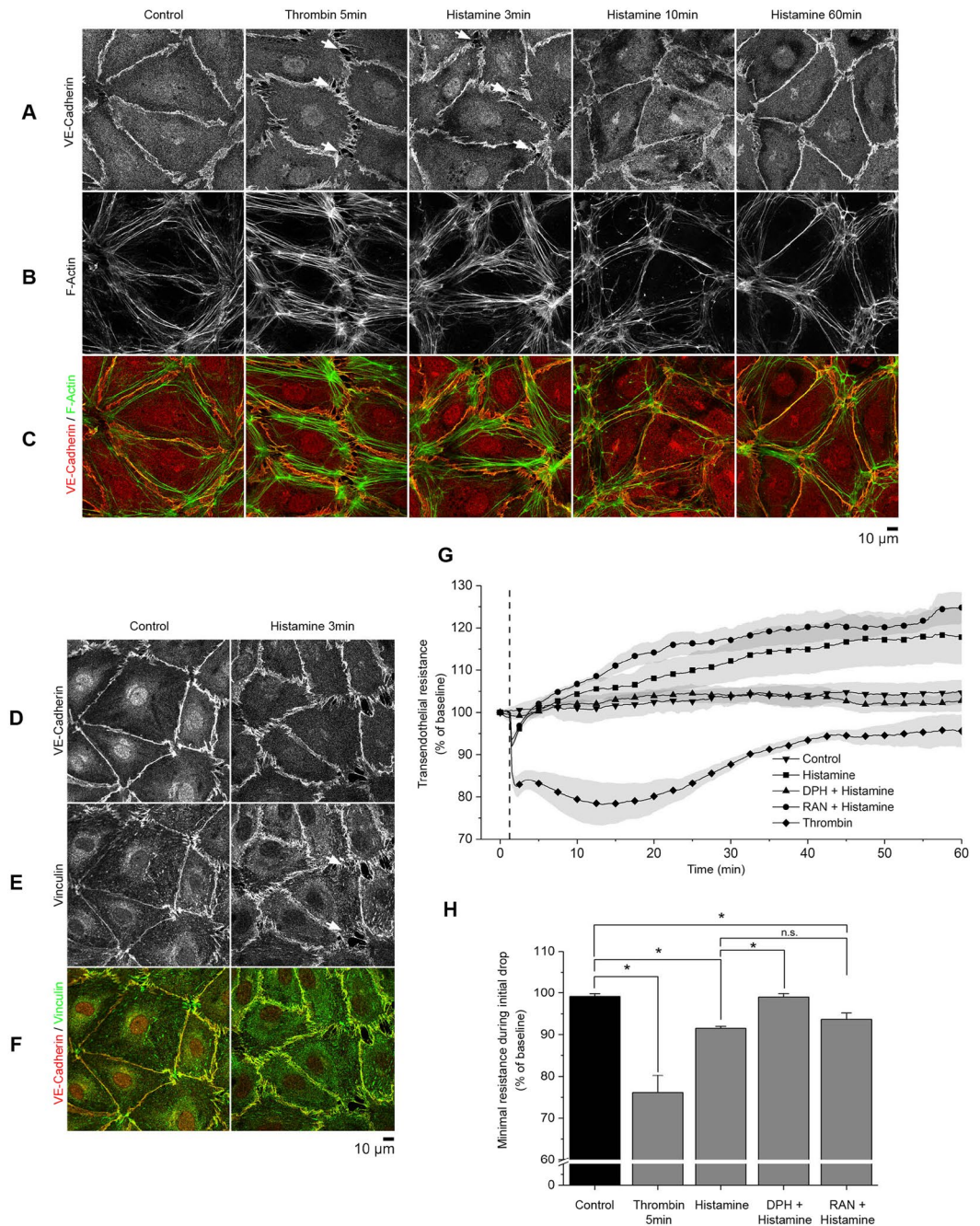


Figure 1. Changes in endothelial morphology and barrier integrity induced by inflammatory mediators. Confluent HDMEC monolayers were incubated with either histamine or thrombin and subsequently fixed with PFA (representative images of $n = 4$ independent experiments). (A–C) Immunostaining against VE-cadherin and F-actin. Histamine and thrombin induced gap formation as indicated by VE-cadherin staining (arrows) and increased stress fiber formation after 3 and 5 min, respectively. At 60 min, stress fiber formation was largely abolished. (D–F) Co-staining for VE-cadherin and vinculin under control conditions and after incubation with histamine for 3 min. Vinculin was visible at the membrane under both conditions, however gap formation was present only upon histamine treatment (arrow). (G) TER measurements in confluent HDMECs after histamine or thrombin stimulation with or without pre-incubation with diphenhydramine (DPH) or ranitidine (RAN) for 60 min ($n = 4$ independent experiments, $*p < 0.05$, dotted line indicates application of mediators). (H) Quantification of minimal resistance during the initial drop showed decreases in basal resistance to $93.5 \pm 0.8\%$ (histamine) and $78.6 \pm 3.7\%$ (thrombin). Pre-incubation with DPH reduced the drop significantly to $98.6 \pm 0.9\%$ whereas pre-incubation with RAN had no significant effect.

no significant changes in Rac1 activity were detected (Fig. 3C,D). As cAMP levels allegedly contribute to barrier breakdown and recovery^{20,33}, intracellular cAMP levels were measured by ELISA. However, no significant changes in cAMP concentrations were detected during the course of barrier breakdown and recovery (Fig. 3G).

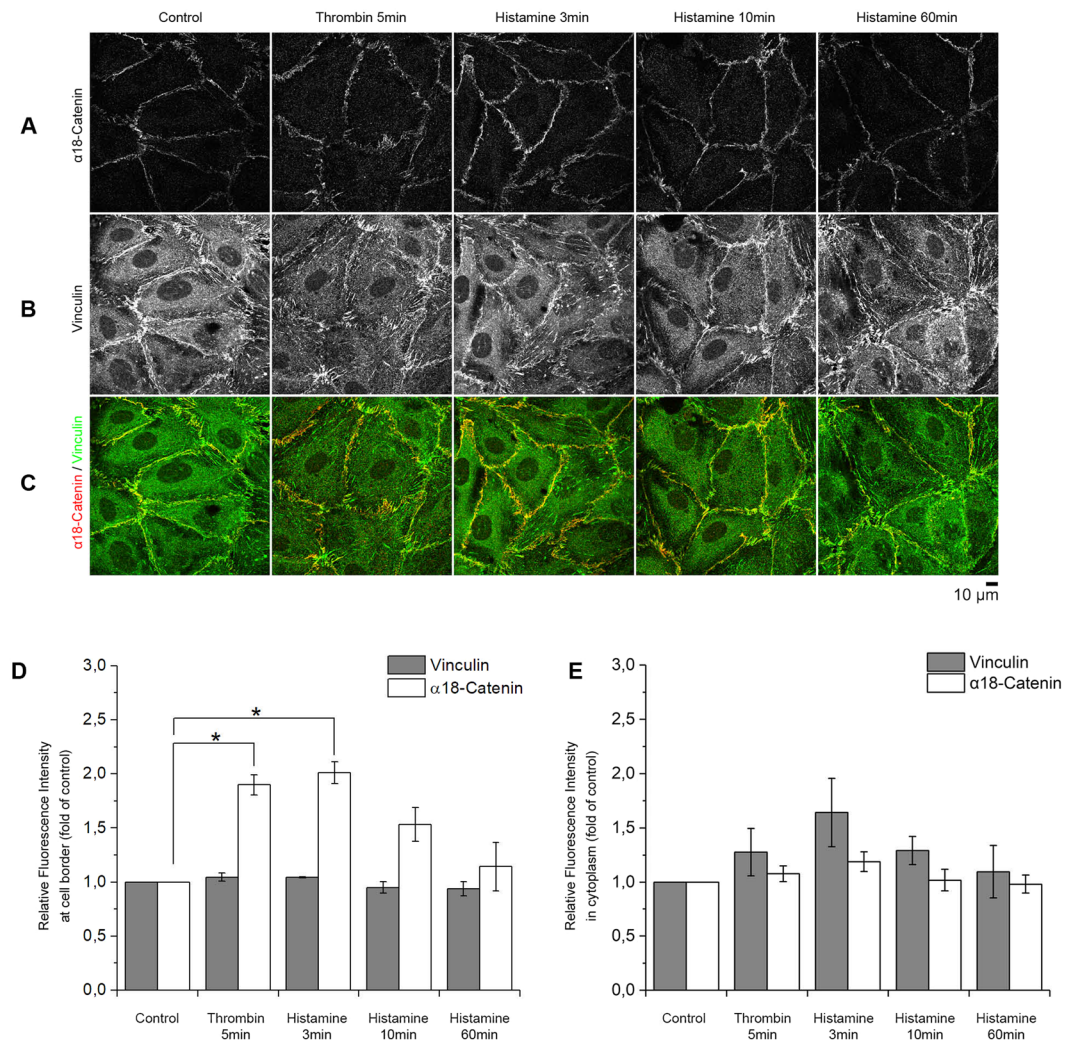


Figure 2. α18-catenin staining along AJs. (A–C) Staining with antibodies against α18-catenin and vinculin after the addition of histamine or thrombin at different time-points. (D) Automated quantification of the fluorescence intensity at the cell border after staining with α18-catenin or vinculin using CellProfiler. Intensity of α18-catenin staining increased significantly 3 and 5 min after addition of histamine or thrombin, respectively (n = 4 independent experiments, *p < 0.05). At these time points intensity of vinculin staining did not change significantly at the membrane. (n = 4 independent experiments, *p < 0.05) The relative fluorescent intensity of vinculin in the cytoplasm was slightly increased upon thrombin and histamine treatment while under the same conditions α18-catenin was unaltered. (n = 4 independent experiments, *p < 0.05).

After activation of the histamine type 1 receptor, downstream activation of PLC-β leads to increased intracellular Ca²⁺ concentrations, subsequently activating a cascade of signaling molecules^{23,34,35}. Ratiometric FURA measurements³⁶ were used to determine the Ca²⁺-concentration in HDMEC monolayers after histamine or thrombin stimulation. Both mediators lead to a strong Ca²⁺ influx that correlated with force production. Preincubation with DPH abrogated this influx, whereas the histamine type 2 receptor inhibitor RAN did not (Fig. 3E,F).

Histamine and thrombin cause activation of RhoA along cell junctions. To further investigate the signaling patterns involved in histamine-induced inflammation, we used fluorescence resonance energy probes to elucidate the subcellular localization of GTP-bound RhoA³². Primary microvascular endothelial cells (HDMEC) were transfected with Raichu-RhoA plasmid and allowed 24 h of rest for stable expression of the Förster Resonance Energy Transfer (FRET) probes. Under basal conditions, the probe localized primarily to the membrane, but was also detectable throughout the cytosol (Fig. 4A). Consistent with the GLISA experiments, in the whole cell histamine and thrombin both increased the absolute FRET efficiency to 263.8% ± 29.5% and 262.0% ± 19.3% of control after 3 and 5 min, respectively (Fig. 4B). Furthermore, RhoA activity at the membrane was measured by averaging the FRET efficiency over the outermost ten pixels of the cell (Fig. 4C). We detected activation to 263.1% ± 30.0% and 252.2% ± 23.0% of control at the cell border after addition of histamine and thrombin, respectively. At the 10 and 60 min time points of histamine treatment, FRET efficiency no longer differed significantly from control.

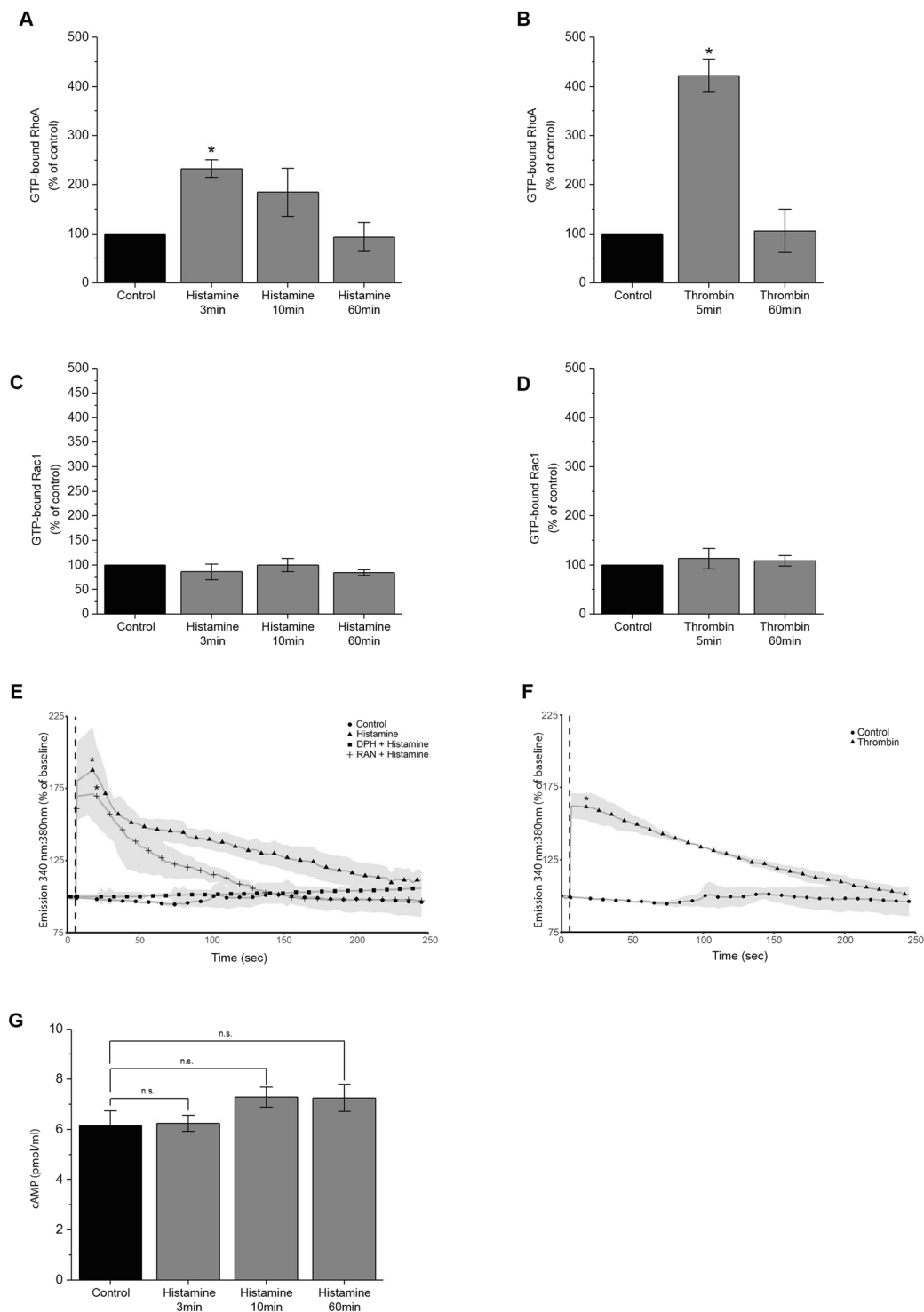


Figure 3. Signaling pathways activated during histamine-mediated barrier disruption. (A,B) RhoGTPase ELISA (GLISA) measurements of HDMECs after incubation with histamine or thrombin at different time points. In comparison to the control, RhoA activity increased significantly 3 and 5 min after addition of histamine or thrombin, respectively ($n = 4$ independent experiments, $*p < 0.05$). (C,D) No changes of Rac1 activity, measured by GLISA, were observed upon different treatments ($n = 3$ independent experiments, $*p < 0.05$). (E) Fluorescence intensity measurements of FURA-2-AM revealed a significant increase in intracellular Ca^{2+} concentration following histamine stimulation. Pre-incubation with DPH but not RAN completely abolished Ca^{2+} influx ($n = 5$ independent experiments, $*p < 0.05$, dotted line indicates histamine application). (F) FURA-2-AM measurements after thrombin stimulation showed a similar burst in intracellular Ca^{2+} levels ($n = 4$ independent experiments, $*p < 0.05$, dotted line indicates addition of thrombin). (G) Measurement of intracellular cAMP concentration after histamine treatment revealed no significant change of cAMP levels ($n = 4$, $*p < 0.05$).

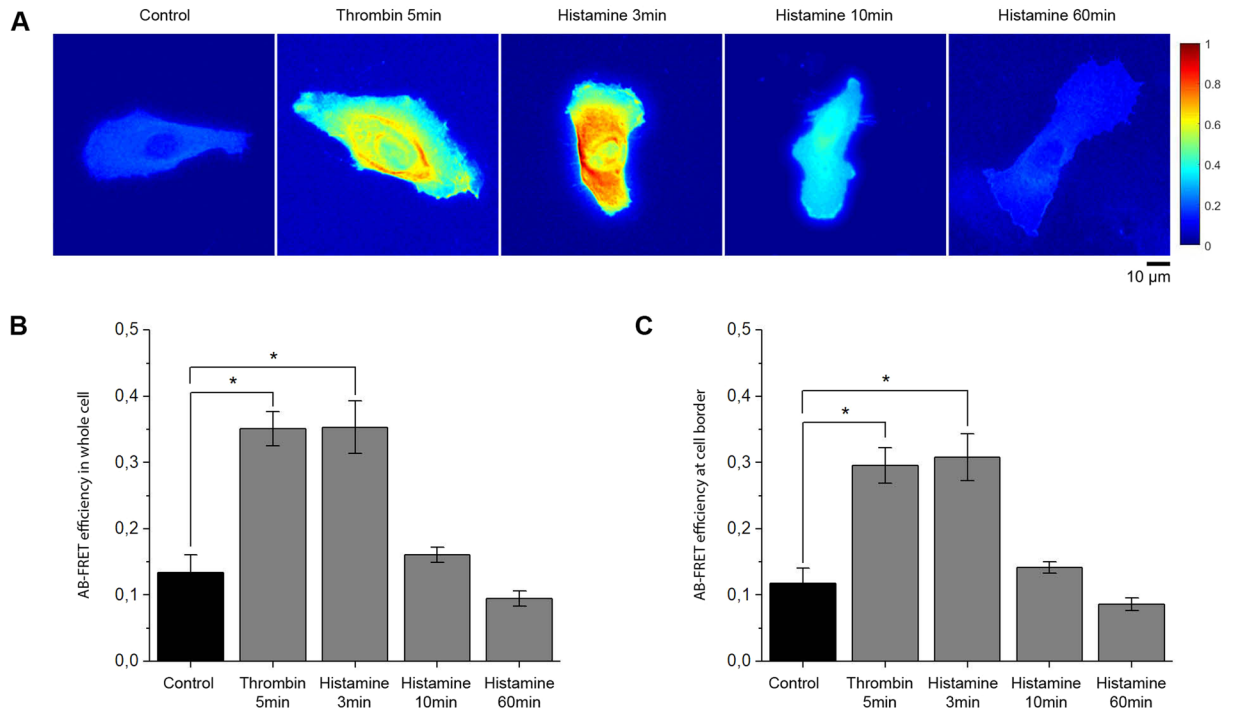


Figure 4. Histamine and thrombin induce activation of RhoA at cell borders. Acceptor-photobleaching FRET efficiency in HDMECs transfected with Raichu-RhoA probes and treated with either histamine or thrombin. (A) Pseudocolor representation of the absolute FRET efficiency showed localization of active RhoA in the whole cell (representative images of $n = 5$ independent experiments). (B,C) The mean absolute FRET efficiency quantified over the whole cell and cell borders using CellProfiler ($n = 5$ independent experiments, $*p < 0.05$). Incubation with thrombin (5 min) and histamine (3 min) significantly increased RhoA activity in the whole cell as well as at the cell border. ($n = 5$ independent experiments, $*p < 0.05$).

Inhibition of ROCK and Ca^{2+} -signaling reduces histamine-induced barrier dysfunction and α 18-catenin staining. Downstream of histamine receptor activation, intracellular Ca^{2+} -signaling and Rho Kinase (ROCK) activation contribute to endothelial barrier dysfunction^{27,28}. Y27632, a specific inhibitor of ROCK I and ROCK II and BAPTA-AM, an intracellular Ca^{2+} -chelator, were used to suppress these pathways. Primary microvascular endothelial cells were preincubated with Y27632 or BAPTA-AM before histamine or thrombin addition and stained for VE-cadherin and F-actin (Fig. 5A–C, Supplementary Fig. S2A–C). Both Ca^{2+} -chelation and ROCK inhibition prevented AJ disruption. Interestingly, BAPTA-AM effectively abrogated stress fiber formation whereas Y27632 did not, suggesting that Ca^{2+} -dependent and Rho-independent pathways may also be involved. The results were confirmed by TER measurements (Fig. 5D). The drop in TER after the addition of histamine was inhibited by incubation with both BAPTA-AM (maximum drop $99.4 \pm 0.3\%$ of baseline) and Y27632 (maximum drop $98.1 \pm 1.8\%$) (Fig. 5E). However, GLISA experiments showed that preincubation with BAPTA-AM significantly reduced RhoA activation in response to histamine to $127.9 \pm 14.4\%$ of control compared to $197.2 \pm 24.06\%$ after incubation with histamine alone for 3 min, suggesting that Ca^{2+} -signaling is required for full activation of RhoA (Fig. 5F).

Next, we studied the effect of ROCK inhibition and Ca^{2+} -signaling on α 18-catenin staining intensity along cell borders (Fig. 6A). The mean relative intensity in α 18-catenin staining at cell borders after histamine incubation ($161.2 \pm 18.5\%$) was reduced by preincubation with Y27632 ($106.2 \pm 18.2\%$) and BAPTA-AM ($99.6 \pm 19.7\%$) (Fig. 6D). Notably, the intensity of vinculin staining at junctions as well as colocalization with α 18-catenin did not change significantly (Fig. 6B,D,E, Supplementary Fig. S1C). In addition, similar to Fig. 2 histamine induced a dotted staining pattern of vinculin resembling focal adhesions which was reflected in an inconsistent but not significant increase of vinculin staining intensity in the cytoplasm and also was abrogated by and BAPTA-AM.

Histamine disrupts actin and vinculin localization along endothelial membranes *in vivo*. To test whether the aforementioned effects of histamine also occur *in vivo*, the experimental conditions were replicated in a rat model. We used the modified Landis technique¹, in which a single postcapillary venule of rat mesentery was cannulated with a glass capillary and continuously perfused with ringer solution containing BSA to dilute erythrocytes to visualize flow. After 5 min of perfusion with either control or histamine-containing solution the rat was euthanized, and the mesentery was immediately fixed with formaldehyde. The injected and marked venules were immunostained for vinculin together with F-actin labeling. Unfortunately, α 18-catenin staining was not feasible since the antibodies origin is rat. Of note, parallel experiments using thrombin were not possible since it is known that intact mesenteric venules do not respond to thrombin^{37,38}. Under control conditions, we observed

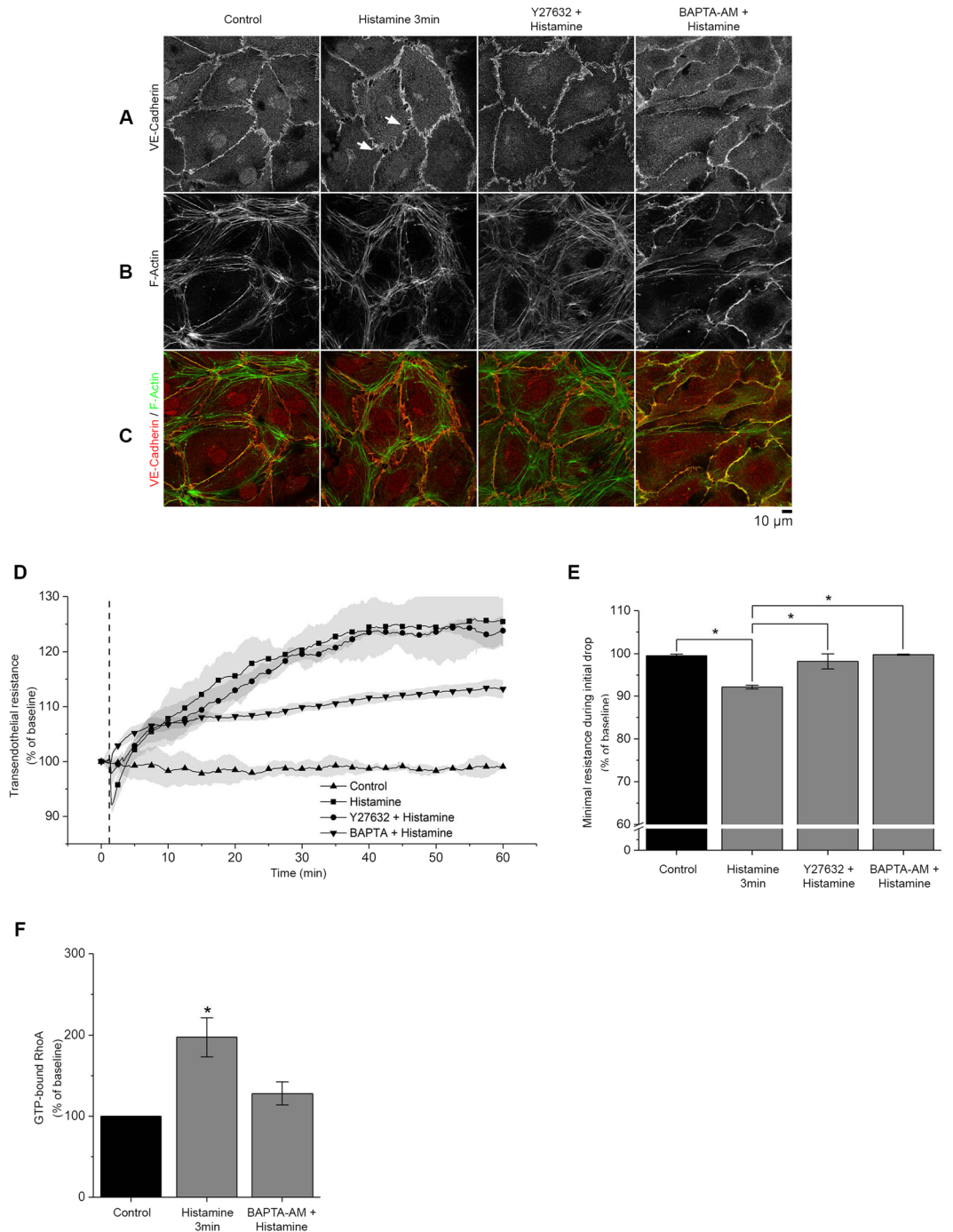


Figure 5. Inhibition of ROCK and Ca^{2+} signaling reduces histamine-induced barrier dysfunction. (A–C) Staining of HDMEC monolayers against VE-cadherin and F-actin after stimulation with histamine alone or after pre-incubation with either Y27632 (30 min) or BAPTA-AM (2 h). The gaps (arrows) induced by histamine (3 min) were largely abolished by application of either Y27632 or BAPTA-AM ($n = 4$ independent experiments). (D,E) TER measurements showed that the initial drop in resistance, induced by histamine, was significantly abolished by pre-incubation with both mediators ($n = 3$ independent experiments, $*p < 0.05$). (F) RhoA GLISA measurements in HDMECs revealed that BAPTA-AM reduces RhoA activation after histamine stimulation. ($n = 3$ independent experiments, $*p < 0.05$ vs control).

colocalization of actin and vinculin along the endothelial cell membranes (Fig. 7). Endothelial cell borders were smooth and parallel to the flow direction. After perfusion with histamine for 5 min, vinculin staining alongside the endothelial cell borders changed to a more ragged appearance (Fig. 7A–C). These results indicate that similar to primary cultured endothelium, vinculin was present at cell borders under resting conditions. Upon histamine treatment, we observed a trend towards lower colocalization of vinculin and filamentous actin as measured by Pearson's correlation coefficient, which however was not significant (Fig. 7D).

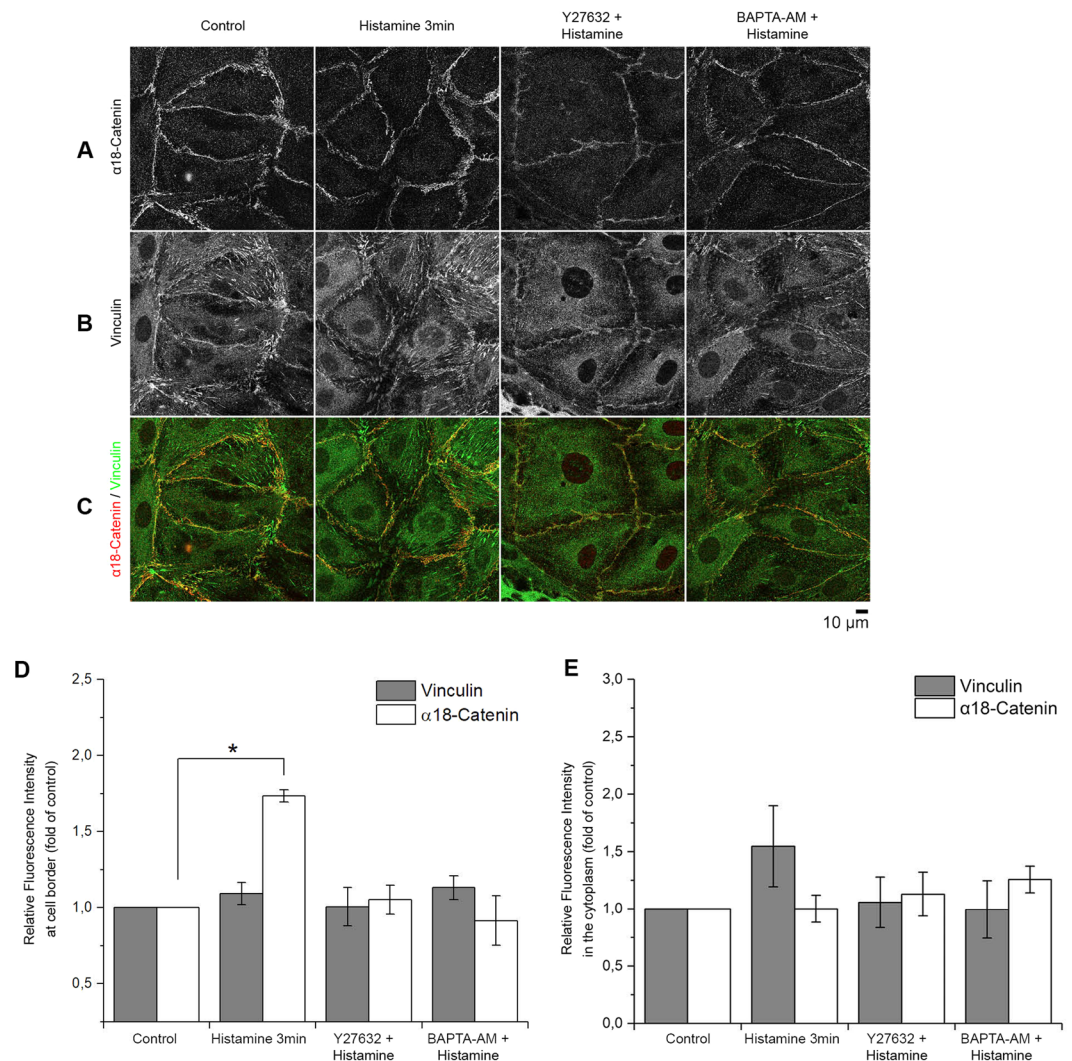


Figure 6. Increased $\alpha 18$ -catenin staining along AJ is dependent on ROCK and intercellular Ca^{2+} signaling. (A–D) In HDMECs co-staining against $\alpha 18$ -catenin and vinculin revealed a marked increase in $\alpha 18$ -catenin staining intensity at cell borders following histamine incubation (3 min). However, this was not the case after pre-incubation with Y27632 or BAPTA-AM ($n = 3$ independent experiments). (D,E) Bar graph showing automated quantification of vinculin and $\alpha 18$ -catenin fluorescence intensity at cell border and in the cytoplasm. Vinculin staining showed no significant change in localization or intensity after pre-incubation with Y27632 or BAPTA-AM. ($n = 3$ independent experiments, $*p < 0.05$).

Discussion

Histamine induces a transient decrease in barrier function accompanied by increased $\alpha 18$ -catenin staining along AJs. The signaling mechanisms underlying acute endothelial barrier breakdown under inflammatory conditions are not entirely clear. Histamine and thrombin induce acute break-down of the endothelial barrier. However, thrombin is not a typical inflammatory mediator since it regulates vascular permeability during the coagulation phase after injury³⁹ and in many studies macrovascular endothelial cells were used, which are good models for investigating adaptations to shear stress but not the inflammatory response, which occurs exclusively in postcapillary venules³. Therefore, re-evaluation of all findings using microvascular endothelium is necessary. Histamine impaired the integrity of the endothelial barrier *in vitro* and *in vivo*^{23,40–42}. The mechanism by which histamine leads to the disruption of the endothelial barrier is not fully understood, however, H1R G α_q -coupled receptors^{27,42,43} and PCK-, RhoA/ROCK- and NO-signaling seem to be important. In addition, histamine has been proposed to disrupt AJs, leading to the rapid formation of a new junction type referred to as focal adherens junction (FAJ), which is characterized by recruitment of vinculin¹⁶.

In this study, we used histamine to study barrier disruption and the corresponding signaling pathways involved in anaphylaxis in primary human microvascular endothelial cells *in vitro* and postcapillary venules of rat mesentery *in vivo*. Thrombin was used in comparison *in vitro* only because intact mesenteric venules do not respond to thrombin^{37,38}. Consistent with the literature⁴², our data showed that histamine and thrombin disrupted the endothelial barrier transiently and caused reduced TER and intercellular gap formation. At the same time, both thrombin and

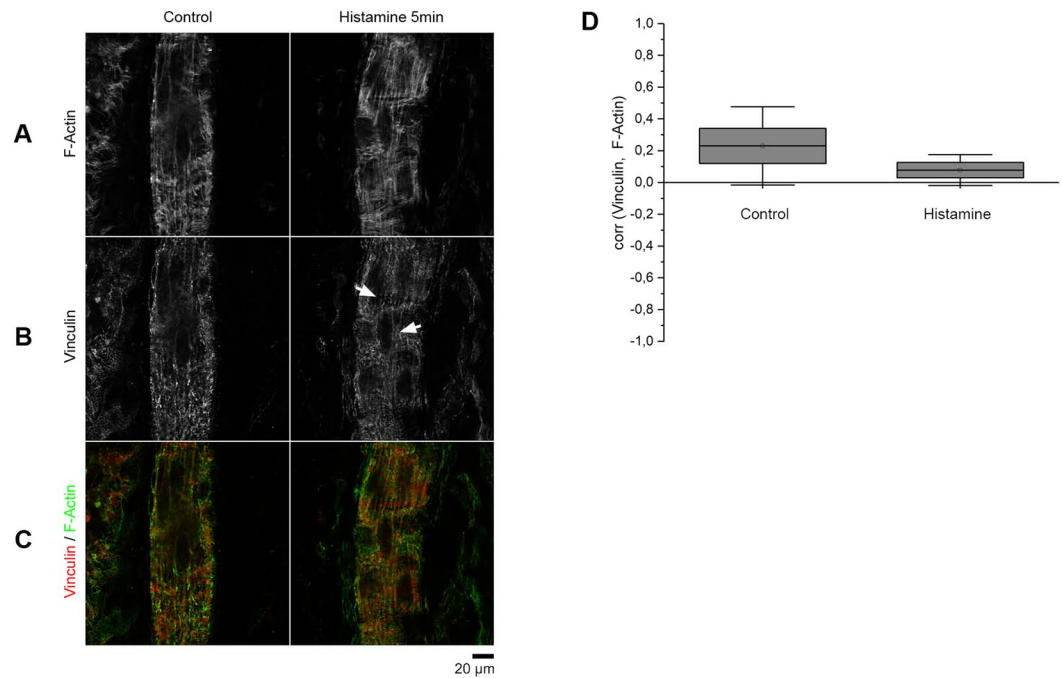


Figure 7. *Ex-vivo* immunostaining of single-perfused rat postcapillary venules demonstrate disruption of vinculin staining along the membrane after histamine stimulation. **(A)** In postcapillary venules actin forms longitudinal fiber bundles. **(B)** Endothelial cells display vinculin staining under resting conditions while the staining along cell borders is disturbed after stimulation with histamine (arrow). **(C)** Overlay of F-actin and vinculin staining ($n = 4$ independent experiments). **(D)** Co-localization between vinculin and actin, determined by Pearson's correlation coefficient, appears to be slightly reduced due to histamine treatment ($n = 4$ independent experiments).

histamine enhanced staining with the conformation-sensitive antibody targeting the alpha 18-subunit of catenin which has been proposed to correlate with increased tension at AJs (Fig. 8). Increased tension may result from RhoA-dependent up-regulation of actomyosin contraction²⁷ which may trigger relocalization of vinculin to AJs from FAJs¹⁶. Therefore, we correlated the different events during endothelial barrier breakdown with immunostaining for vinculin, which is known to be a mechanotransducer with the ability to stabilize adhesion under force^{16,44–46}. Interestingly, we observed that vinculin was localized at cell junctions under resting conditions both in HDMECs *in vitro* and endothelial cells of postcapillary venules *in vivo*. Moreover, after incubation with either histamine or thrombin, vinculin distribution paralleled VE-cadherin and F-actin localization. AJs similar to vinculin were reorganized from continuous linear distribution towards a fragmented staining pattern with perpendicular arrays which were previously described as FAJ. However, the staining intensity for vinculin remained unaffected. These data indicate that in microvascular endothelium, vinculin is a normal constituent of AJs under resting conditions (Fig. 8) and that the term FAJ may not be adequate in this cell type. The discrepancy to the previous study¹⁶ may be explained at least in part by the fact that most experiments in the previous study were shown for HUVECs which is a macrovascular endothelial cell type from fetal tissue and therefore is not derived from the typical vascular bed to study the inflammatory response. Moreover, the confluency of the endothelium, which was maximal under the conditions used for our study, may also have been different. The fact that the microvascular human HDMEC cells exhibited vinculin localization along cell borders similar to endothelial cells of intact post-capillary venules indicates that the conditions used here were appropriate to study endothelial barrier regulation.

RhoA is activated along intercellular junctions whereas no significant change in Rac1 activity or cAMP levels were detected.

Thrombin can increase endothelial permeability by activating Ca^{2+} -/RhoA-signaling, which disrupts endothelial adherens junctions⁴⁷. Similarly, several studies have shown the importance of RhoA signalling in histamine-induced leakage. Most recently, RhoA-deficient animals were protected against histamine-induced vascular permeability^{26,47}. Our results support this notion (Fig. 8) since inhibition of ROCK effectively blocked histamine-induced barrier breakdown. However, how RhoA signaling induces the disruption of the endothelial barrier is less well defined. Because activation of RhoA GTPase is spatiotemporally controlled²⁶ and overall activation as shown by GLISA may not accurately reflect activation at the site of cell junctions, we used Rho GTPase FRET sensors to visualize activation with high temporal and spatial resolution. These sensors change conformation and subsequent FRET efficiency depending on the local balance of guanine nucleotide exchange factors (GEFs) and GTPase-activating proteins (GAPs). Our data confirm that treatment with both thrombin or histamine induced activation of RhoA in the cytoplasm and also along cell borders. This is in line with the idea that RhoA has an important role in the regulation of endothelial barrier properties after treatment with inflammatory mediators.

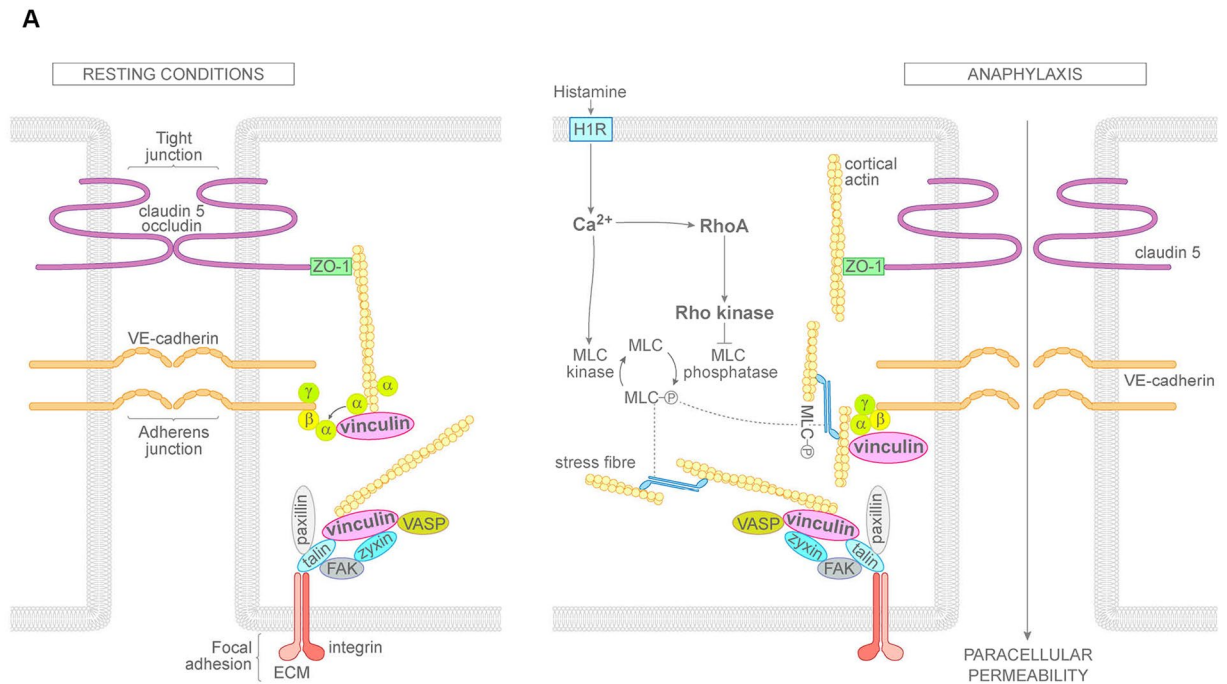


Figure 8. Mechanisms of histamine-induced endothelial barrier disruption. Under resting conditions, vinculin is localized mainly along endothelial cell borders and at least in part co-localizes with VE-cadherin and α -catenin at AJs. In anaphylaxis, histamine induces a rapid increase of cytoplasmic Ca^{2+} leading to activation of RhoA. Both events induce stress fiber formation at focal adhesions. In addition, RhoA via Rho kinase may enhance tension on α -catenin at endothelial AJs which causes AJ reorganization. H1R = Histamine receptor type I; Ca^{2+} = calcium; MLC = myosin light chain; FAK = focal adhesion kinase; VASP = vasodilator-stimulated phosphoprotein; ZO-1 = zonula occludens protein 1; α , β , γ = α -, β -, γ -catenin; ECM = extracellular matrix.

In addition, it is well established that activated small GTPase Rac1 and the second messenger cAMP stabilize endothelial barrier properties⁴⁸. For LPS and $\text{TNF-}\alpha$, it has been shown that endothelial barrier breakdown temporally was closely associated with both decreased cAMP levels and Rac1 inactivation whereas RhoA activation was observed later^{48,49}. Moreover, CNF-1 under conditions where it activated Rac1 and RhoA in parallel in cultured endothelium was effective to abrogate $\text{TNF-}\alpha$ -induced barrier breakdown in mesenteric post-capillary venules *in vivo* whereas Rho kinase inhibition was not. These observations suggest that inactivation of Rac1 rather than stimulation of the RhoA/Rho kinase pathway was the primary mechanism underlying $\text{TNF-}\alpha$ -mediated permeability increase.

Surprisingly, our results of the present study showed no differences in Rac1 activity or in cAMP concentrations after treatment with histamine. Therefore, we conclude that in contrast to the situation in sepsis, where LPS and $\text{TNF-}\alpha$ are relevant, alterations of cAMP levels as well as Rac1 activity are less important in anaphylaxis. Rather, acute inflammation appears to be primarily dependent on Ca^{2+} and activation of RhoA.

Ca^{2+} signaling is required for RhoA activation, AJ reorganization and barrier dysfunction.

Permeability mediators, including histamine, act on G_{Oq} -coupled GPCRs leading the activation of PLC- β and the rapid mobilization of Ca^{2+} , which promotes MLC phosphorylation and the stimulation of its contractile activity²⁷. RhoA can be activated independently by H1R coupled to $\text{G}_{\text{q/11}}$ ²⁸. H1R also leads to an increase of intracellular Ca^{2+} concentration. As reported previously²⁸, we found that H1 receptor is required for histamine to induce permeability (Fig. 8). Our results revealed that both histamine and thrombin lead to a rapid Ca^{2+} -influx accompanied by parallel reduction of TER. Chelation of Ca^{2+} by BAPTA-AM similar to inhibition of ROCK blocked the effects of histamine and thrombin on barrier function and AJ reorganization. Moreover, BAPTA-AM prevented activation of RhoA and similar to inhibition of ROCK blunted α 18-catenin staining along junctions. These results indicate that Ca^{2+} -mediated RhoA activation is critical for endothelial barrier regulation (Fig. 8). The pivotal role of RhoA has been demonstrated previously²⁷, however, in this study the authors concluded that RhoA was activated primarily independent of Ca^{2+} . In addition, we observed that stress fiber formation in response to histamine was abrogated by chelation of Ca^{2+} but not by inhibition of Rho kinase. This supports the notion that in response to histamine stress fiber formation can be induced by Ca^{2+} in a manner independent of Rho kinase, most likely via MLCK⁵⁰, and suggests that stress fibers are not directly involved in tension formation at AJ and endothelial barrier breakdown (Fig. 8).

Conclusion

Therefore, we conclude that Ca^{2+} via RhoA/ROCK activation is critical for histamine-induced barrier disruption which correlated with tension-associated α 18-catenin staining along endothelial AJ. These data suggests that the patterns of signaling mechanisms engaged in acute inflammatory barrier disruption differ to more delayed responses as seen in sepsis where reduction of endothelial cAMP and inactivation of Rac1 appears to be more relevant². Furthermore, Rho-mediated tension may be involved in acute endothelial barrier disruption, at least *in vitro*.

Methods

Cell Culture and antibodies. All experiments were performed using Human Dermal Microvascular Endothelial Cells (HDMEC) (Promocell, Heidelberg, Germany). Cells were maintained in corresponding medium (Endothelial Cell Growth Medium MV; Promocell, Heidelberg, Germany) and used at passages between three and six. Vascular endothelial (VE-) cadherin was detected using goat-anti-VE-cadherin antibody purchased from Santa Cruz Biotechnology (Santa Cruz, USA). Vinculin was immunostained using mouse- α -vinculin antibody purchased from Abcam (Cambridge, UK). Rat α 18-catenin antibody was contributed from Yonemura S. (RIKEN Center for Developmental Biology, Kobe, Hyogo, Japan)³⁰. Filamentous actin (F-actin) was illuminated using an Alexa 488 phalloidin dye (Life Technologies, Karlsruhe, Germany). The addition of 4',6'-diamidino-2-phenylindole (DAPI) was used to assess nuclear morphology. Corresponding secondary antibodies were purchased from Dianova (Hamburg, Germany) and were also used for control experiments (Supplementary Fig. S3).

Test Reagents. Histamine and thrombin were purchased from Sigma-Aldrich (Munich, Germany). Histamine was used at 10 μM for the indicated times and thrombin was used at 10 U for 5 min. BAPTA-AM (Sigma-Aldrich, Germany) was preincubated for two hours at 5 μM . Diphenhydramine was used to inhibit activation of histamine receptor type I, and ranitidine was used for inhibition of histamine receptor type II. Both were preincubated at 1 μM and 10 μM , respectively, for 15 min. The ROCK inhibitor Y27632 (Sigma-Aldrich, Germany) was preincubated for 30 min at 10 μM .

Transendothelial Electric Resistance Measurements. The barrier integrity of HDMECs was measured using an ECIS Z Theta system (Applied Biophysics, New York, U.S.A). HDMEC monolayers were grown to confluence on uncoated 8W10E electrodes. Immediately before the experiment, the medium was exchanged and the electrode was mounted on a holder inside an incubator at 37 °C with 5% CO_2 . Transendothelial resistance was measured at 4000 Hz every 10 seconds. Test reagents were diluted in pre-warmed medium. After recording 5 min of baseline values, the mediators were added.

Immunostaining. HDMECs were grown to confluence on uncoated glass cover slips, treated with vehicle or test reagents and fixed with 4% formaldehyde in PBS for 10 min at room temperature. After washing and permeabilization using 0.1% Triton X-100 in PBS, the cells were blocked with 10% normal goat or donkey serum and 1% BSA in PBS. The respective primary antibody was incubated overnight at 1:100 in PBS at 4 °C. After washing, cells were treated with respective secondary antibodies coupled to Cy2, Cy3 or Cy5 for one hour and then embedded in n-propyl gallate. F-actin was stained using an Alexa 488 phalloidin dye added to the diluted secondary antibody at 1:100. Using the fixation protocol described above, patterns of actin filaments under control conditions resembled those observed in previous studies^{49,51,52}. However, we cannot guarantee that all peripheral filaments were preserved when compared to an unfixed state, which we believe is not important for this study.

Stained monolayers were sequentially illuminated using a Leica SP5 confocal microscope (Mannheim, Germany) with an HCY PL APO Lambda blue 63 \times 1.4 oil immersion objective and a zoom of 2x. Cy3 was illuminated with a wavelength of 542 nm and Cy5 with 633 nm. The same microscope settings were used under all conditions. Secondary antibody controls were performed for all co-immunostainings (Supplementary Fig. S3).

To calculate the Pearson's correlation coefficient confocal images were analysed using Image Processing and Analysis in Java's (Image J) segmented line and plot profile tools. A line (110 pixels length, 2 pixels width) was drawn along cell borders based either on F-actin or vinculin distribution. Subsequently, plot profiles were generated using the built-in tool. Pixel gray values for both proteins of interest obtained from these plots were transferred to Excel and used for calculations of the Pearson's correlation coefficient.

G-Protein ELISA (GLISA)/cAMP-ELISA. Intracellular concentrations of GTP-bound Rac1 and RhoA proteins were determined using commercially available ELISA kits purchased from Cytoskeleton (Denver, U.S.A). The assay was performed according to the manufacturer's instructions. The technique was used as described previously³³, cAMP concentrations were measured by cAMP enzyme linked immunosorbent assay (CA-200) (Sigma-Aldrich, St. Louis, U.S.A.) as described previously⁵³.

Fluorescence Resonance Energy Transfer (FRET). Spatiotemporal activation of RhoA was determined using a RhoA-Ras and interacting protein chimeric unit (Raichu) -probe (a kind gift of Miyazaki J., Kyoto University, Japan)^{54,55} consisting of four modules: a donor (CFP), an acceptor (YFP), a Rho binding domain (RBD) and the Rho GTPase itself. Upon exchange of GDP to GTP, the RBD binds the GTP-RhoA complex and the distance between the donor and acceptor decreases, increasing the energy transfer from the donor to an acceptor when illuminated at donor excitation wavelength. The RhoA-Raichu probe is contained in a transfectable plasmid. The plasmid was transfected with jetPRIME (VWR) into HDMECs at 80% confluence, grown to a confluent monolayer and then subjected to FRET-measurements. After the addition of mediators, the cells were fixed using 4% PFA in PBS for 20 min. Using standard acceptor photobleaching protocol⁵⁶, YFP was bleached for 3 min at 514 nm and CFP intensity was recorded before and after bleaching. Processing was performed in ImageJ and absolute FRET efficiency values were recorded.

FURA-2 AM Measurements. Intracellular Ca^{2+} concentrations were detected by radiometric analysis of FURA-2-AM (Thermo-Fisher, Massachusetts, USA). Cells were incubated in FURA-containing medium for 45 min, and then the medium was exchanged. After a 15 min rest period to allow cleavage of the ester, the cells were illuminated every 3 seconds and the signal was detected at 340 nm/380 nm. After 20 seconds of baseline detection, reagents were added.

Microperfusion of rat venules. We perfused single postcapillary venules in the rat mesentery using the modified Landis technique^{3,57,58}. Wistar rats (provided from Janvier Labs, Saint-Berthevin Cedex) with body weights between 280 g and 350 g were anesthetized by subcutaneous injection of ketamine (60.0–75.0 mg/kg) and medetomidine (0.25–0.5 mg/kg). Then small unbranched microvessels with convergent flow were cannulated using sharp glass micropipettes and perfused continuously with mammalian ringer solution containing 10 mg/ml bovine serum albumin (BSA) with or without 10 μM /l histamine dihydrochloride. Further addition of diluted erythrocyte concentrate allowed visualization of correct placement and flow. After 5 min of perfusion, the rats were euthanized and the intact mesentery was washed and fixed immediately in 4% formaldehyde in PBS. The mesentery was then spread on adhesive glass slides, permeabilized with 0.1% Triton in PBS and blocked using BSA/NDS. Further immunostaining for VE-cadherin, vinculin and F-actin was performed as described above. Illumination was performed by taking z-stacks with a confocal microscope (Leica SP5 confocal microscope) using a 63×1.4 water immersion objective. All rats were kept under conditions that conformed to the regulations of the Regierung von Oberbayern and all experiments were performed in accordance with relevant guidelines and regulations. The experimental protocol was approved by the Regierung von Oberbayern.

Statistics. Immunofluorescence experiments were quantified using CellProfiler (CarpenterLab, Cambridge, USA). After background subtraction, cell borders were segmented and the mean fluorescence intensity recorded⁵⁹. For automated measurements of fluorescence intensity in the cytosol, the area of the segmented cell borders was subtracted from each image and mean intensity was calculated. The data analysis was carried out using R⁶⁰ (R Foundation, Vienna, Austria) and OriginPro 2017 g (OriginLab Corporation, Northampton, USA). Statistical analysis was carried out using one-way ANOVA followed by Holm–Bonferroni corrections for multiple comparisons. All data are presented as the mean \pm standard error of the mean. The results were considered statistically significant at $p < 0.05$.

References

1. Mehta, D. & Malik, A. B. Signaling mechanisms regulating endothelial permeability. *Physiol Rev* **86**, 279–367, <https://doi.org/10.1152/physrev.00012.2005> (2006).
2. Amado-Azevedo, J., Valent, E. T. & Van Nieuw Amerongen, G. P. Regulation of the endothelial barrier function: a filum granum of cellular forces, Rho-GTPase signaling and microenvironment. *Cell Tissue Res* **355**, 557–576, <https://doi.org/10.1007/s00441-014-1828-6> (2014).
3. Michel, C. C. & Curry, F. E. Microvascular permeability. *Physiol Rev* **79**, 703–761 (1999).
4. Michiels, C. Endothelial cell functions. *J Cell Physiol* **196**, 430–443, <https://doi.org/10.1002/jcp.10333> (2003).
5. Radeva, M. Y. & Waschke, J. Mind the gap: mechanisms regulating the endothelial barrier. *Acta Physiol (Oxf)*, <https://doi.org/10.1111/apha.12860> (2017).
6. Trani, M. & Dejana, E. New insights in the control of vascular permeability: vascular endothelial-cadherin and other players. *Curr Opin Hematol* **22**, 267–272, <https://doi.org/10.1097/MOH.0000000000000137> (2015).
7. Schlegel, N. & Waschke, J. cAMP with other signaling cues converges on Rac1 to stabilize the endothelial barrier - a signaling pathway compromised in inflammation. *Cell Tissue Res* **355**, 587–596, <https://doi.org/10.1007/s00441-013-1755-y> (2014).
8. Schnittler, H. *et al.* Actin filament dynamics and endothelial cell junctions: the Ying and Yang between stabilization and motion. *Cell Tissue Res* **355**, 529–543, <https://doi.org/10.1007/s00441-014-1856-2> (2014).
9. Nelson, W. J. Regulation of cell-cell adhesion by the cadherin-catenin complex. *Biochem Soc Trans* **36**, 149–155, <https://doi.org/10.1042/BST0360149> (2008).
10. Bravi, L., Dejana, E. & Lampugnani, M. G. VE-cadherin at a glance. *Cell Tissue Res* **355**, 515–522, <https://doi.org/10.1007/s00441-014-1843-7> (2014).
11. Komarova, Y. & Malik, A. B. Regulation of endothelial permeability via paracellular and transcellular transport pathways. *Annu Rev Physiol* **72**, 463–493, <https://doi.org/10.1146/annurev-physiol-021909-135833> (2010).
12. Abe, K. & Takeichi, M. EPLIN mediates linkage of the cadherin catenin complex to F-actin and stabilizes the circumferential actin belt. *Proc Natl Acad Sci USA* **105**, 13–19, <https://doi.org/10.1073/pnas.0710504105> (2008).
13. Buckley, C. D. *et al.* Cell adhesion. The minimal cadherin-catenin complex binds to actin filaments under force. *Science* **346**, 1254211, <https://doi.org/10.1126/science.1254211> (2014).
14. Takeichi, M. Cadherins: a molecular family important in selective cell-cell adhesion. *Annu Rev Biochem* **59**, 237–252, <https://doi.org/10.1146/annurev.bi.59.070190.001321> (1990).
15. Sukriti, S., Tauseef, M., Yazbeck, P. & Mehta, D. Mechanisms regulating endothelial permeability. *Pulm Circ* **4**, 535–551, <https://doi.org/10.1086/677356> (2014).
16. Huvneers, S. *et al.* Vinculin associates with endothelial VE-cadherin junctions to control force-dependent remodeling. *J Cell Biol* **196**, 641–652, <https://doi.org/10.1083/jcb.201108120> (2012).
17. Leerberg, J. M. & Yap, A. S. Vinculin, cadherin mechanotransduction and homeostasis of cell-cell junctions. *Protoplasma* **250**, 817–829, <https://doi.org/10.1007/s00709-012-0475-6> (2013).
18. Aberle, H., Schwartz, H. & Kemler, R. Cadherin-catenin complex: protein interactions and their implications for cadherin function. *J Cell Biochem* **61**, 514–523, [https://doi.org/10.1002/\(SICI\)1097-4644\(19960616\)61:4<514::AID-JCB4>3.0.CO;2-R](https://doi.org/10.1002/(SICI)1097-4644(19960616)61:4<514::AID-JCB4>3.0.CO;2-R) (1996).
19. Birukova, A. A. *et al.* Selective Role of Vinculin in Contractile Mechanisms of Endothelial Permeability. *Am J Respir Cell Mol Biol* **55**, 476–486, <https://doi.org/10.1165/rcmb.2015-0328OC> (2016).
20. Dejana, E., Orsenigo, F. & Lampugnani, M. G. The role of adherens junctions and VE-cadherin in the control of vascular permeability. *J Cell Sci* **121**, 2115–2122, <https://doi.org/10.1242/jcs.017897> (2008).
21. Birukova, A. A., Shah, A. S., Tian, Y., Moldobaeva, N. & Birukov, K. G. Dual role of vinculin in barrier-disruptive and barrier-enhancing endothelial cell responses. *Cell Signal* **28**, 541–551, <https://doi.org/10.1016/j.cellsig.2016.02.015> (2016).
22. Curry, F. R. & Adamson, R. H. Tonic regulation of vascular permeability. *Acta Physiol (Oxf)* **207**, 628–649, <https://doi.org/10.1111/apha.12076> (2013).

23. Moy, A. B. *et al.* Histamine and thrombin modulate endothelial focal adhesion through centripetal and centrifugal forces. *J Clin Invest* **97**, 1020–1027, <https://doi.org/10.1172/JCI118493> (1996).
24. Waschke, J., Burger, S., Curry, F. R., Drenckhahn, D. & Adamson, R. H. Activation of Rac-1 and Cdc42 stabilizes the microvascular endothelial barrier. *Histochem Cell Biol* **125**, 397–406, <https://doi.org/10.1007/s00418-005-0080-2> (2006).
25. Birukova, A. A., Alekseeva, E., Mikaelyan, A. & Birukov, K. G. HGF attenuates thrombin-induced endothelial permeability by Tiam1-mediated activation of the Rac pathway and by Tiam1/Rac-dependent inhibition of the Rho pathway. *FASEB J* **21**, 2776–2786, <https://doi.org/10.1096/fj.06-7660com> (2007).
26. Spindler, V., Schlegel, N. & Waschke, J. Role of GTPases in control of microvascular permeability. *Cardiovasc Res* **87**, 243–253, <https://doi.org/10.1093/cvr/cvq086> (2010).
27. Mikelis, C. M. *et al.* RhoA and ROCK mediate histamine-induced vascular leakage and anaphylactic shock. *Nat Commun* **6**, 6725, <https://doi.org/10.1038/ncomms7725> (2015).
28. Adderley, S. P., Zhang, X. E. & Breslin, J. W. Involvement of the H1 Histamine Receptor, p38 MAP Kinase, Myosin Light Chains Kinase, and Rho/ROCK in Histamine-Induced Endothelial Barrier Dysfunction. *Microcirculation* **22**, 237–248, <https://doi.org/10.1111/micc.12189> (2015).
29. Schnittler, H. Contraction of endothelial cells: 40 years of research, but the debate still lives. *Histochem Cell Biol* **146**, 651–656, <https://doi.org/10.1007/s00418-016-1501-0> (2016).
30. Yonemura, S., Wada, Y., Watanabe, T., Nagafuchi, A. & Shibata, M. alpha-Catenin as a tension transducer that induces adherens junction development. *Nat Cell Biol* **12**, 533–542, <https://doi.org/10.1038/ncb2055> (2010).
31. Shen, Q., Rigor, R. R., Pivetti, C. D., Wu, M. H. & Yuan, S. Y. Myosin light chain kinase in microvascular endothelial barrier function. *Cardiovasc Res* **87**, 272–280, <https://doi.org/10.1093/cvr/cvq144> (2010).
32. Szulceck, R. *et al.* Localized RhoA GTPase activity regulates dynamics of endothelial monolayer integrity. *Cardiovasc Res* **99**, 471–482, <https://doi.org/10.1093/cvr/cvt075> (2013).
33. Waschke, J., Drenckhahn, D., Adamson, R. H., Barth, H. & Curry, F. E. cAMP protects endothelial barrier functions by preventing Rac-1 inhibition. *Am J Physiol Heart Circ Physiol* **287**, H2427–2433, <https://doi.org/10.1152/ajpheart.00556.2004> (2004).
34. Griner, E. M. & Kazanietz, M. G. Protein kinase C and other diacylglycerol effectors in cancer. *Nat Rev Cancer* **7**, 281–294, <https://doi.org/10.1038/nrc2110> (2007).
35. Hubbard, K. B. & Hepler, J. R. Cell signalling diversity of the Gqalpha family of heterotrimeric G proteins. *Cell Signal* **18**, 135–150, <https://doi.org/10.1016/j.cellsig.2005.08.004> (2006).
36. Russell, J. T. Imaging calcium signals *in vivo*: a powerful tool in physiology and pharmacology. *Br J Pharmacol* **163**, 1605–1625, <https://doi.org/10.1111/j.1476-5381.2010.00988.x> (2011).
37. Curry, F. E., Zeng, M. & Adamson, R. H. Thrombin increases permeability only in venules exposed to inflammatory conditions. *Am J Physiol Heart Circ Physiol* **285**, H2446–2453, <https://doi.org/10.1152/ajpheart.00262.2003> (2003).
38. Kim, M. H., Curry, F. R. & Simon, S. I. Dynamics of neutrophil extravasation and vascular permeability are uncoupled during aseptic cutaneous wounding. *Am J Physiol Cell Physiol* **296**, C848–856, <https://doi.org/10.1152/ajpcell.00520.2008> (2009).
39. Dejana, E. Endothelial cell-cell junctions: happy together. *Nat Rev Mol Cell Biol* **5**, 261–270, <https://doi.org/10.1038/nrm1357> (2004).
40. Leach, L., Eaton, B. M., Westcott, E. D. & Firth, J. A. Effect of histamine on endothelial permeability and structure and adhesion molecules of the paracellular junctions of perfused human placental microvessels. *Microvasc Res* **50**, 323–337, <https://doi.org/10.1006/mvre.1995.1062> (1995).
41. van Nieuw Amerongen, G. P., Draijer, R., Vermeer, M. A. & van Hinsbergh, V. W. Transient and prolonged increase in endothelial permeability induced by histamine and thrombin: role of protein kinases, calcium, and RhoA. *Circ Res* **83**, 1115–1123 (1998).
42. Ashina, K. *et al.* Histamine Induces Vascular Hyperpermeability by Increasing Blood Flow and Endothelial Barrier Disruption *In Vivo*. *PLoS One* **10**, e0132367, <https://doi.org/10.1371/journal.pone.0132367> (2015).
43. Guo, M., Breslin, J. W., Wu, M. H., Gottardi, C. J. & Yuan, S. Y. VE-cadherin and beta-catenin binding dynamics during histamine-induced endothelial hyperpermeability. *Am J Physiol Cell Physiol* **294**, C977–984, <https://doi.org/10.1152/ajpcell.90607.2007> (2008).
44. Dorland, Y. L. & Huvneers, S. Cell-cell junctional mechanotransduction in endothelial remodeling. *Cell Mol Life Sci* **74**, 279–292, <https://doi.org/10.1007/s00018-016-2325-8> (2017).
45. Grashoff, C. *et al.* Measuring mechanical tension across vinculin reveals regulation of focal adhesion dynamics. *Nature* **466**, 263–266, <https://doi.org/10.1038/nature09198> (2010).
46. Carisey, A. *et al.* Vinculin regulates the recruitment and release of core focal adhesion proteins in a force-dependent manner. *Curr Biol* **23**, 271–281, <https://doi.org/10.1016/j.cub.2013.01.009> (2013).
47. van Nieuw Amerongen, G. P., van Delft, S., Vermeer, M. A., Collard, J. G. & van Hinsbergh, V. W. Activation of RhoA by thrombin in endothelial hyperpermeability: role of Rho kinase and protein tyrosine kinases. *Circ Res* **87**, 335–340 (2000).
48. Schlegel, N. & Waschke, J. Impaired cAMP and Rac 1 signaling contribute to TNF-alpha-induced endothelial barrier breakdown in microvascular endothelium. *Microcirculation* **16**, 521–533, <https://doi.org/10.1080/10739680902967427> (2009).
49. Schlegel, N., Baumer, Y., Drenckhahn, D. & Waschke, J. Lipopolysaccharide-induced endothelial barrier breakdown is cyclic adenosine monophosphate dependent *in vivo* and *in vitro*. *Crit Care Med* **37**, 1735–1743, <https://doi.org/10.1097/CCM.0b013e31819deb6a> (2009).
50. Sheldon, R., Moy, A., Lindsley, K., Shasby, S. & Shasby, D. M. Role of myosin light-chain phosphorylation in endothelial cell retraction. *Am J Physiol* **265**, L606–612, <https://doi.org/10.1152/ajplung.1993.265.6.L606> (1993).
51. Kugelmann, D., Waschke, J. & Radeva, M. Y. Adducin is involved in endothelial barrier stabilization. *PLoS One* **10**, e0126213, <https://doi.org/10.1371/journal.pone.0126213> (2015).
52. Baumer, Y., Drenckhahn, D. & Waschke, J. cAMP induced Rac 1-mediated cytoskeletal reorganization in microvascular endothelium. *Histochem Cell Biol* **129**, 765–778, <https://doi.org/10.1007/s00418-008-0422-y> (2008).
53. Spindler, V., Vielmuth, F., Schmidt, E., Rubenstein, D. S. & Waschke, J. Protective endogenous cyclic adenosine 5'-monophosphate signaling triggered by pemphigus autoantibodies. *J Immunol* **185**, 6831–6838, <https://doi.org/10.4049/jimmunol.1002675> (2010).
54. Itoh, R. E. *et al.* Activation of rac and cdc42 video imaged by fluorescent resonance energy transfer-based single-molecule probes in the membrane of living cells. *Mol Cell Biol* **22**, 6582–6591 (2002).
55. Niwa, H., Yamamura, K. & Miyazaki, J. Efficient selection for high-expression transfectants with a novel eukaryotic vector. *Gene* **108**, 193–199 (1991).
56. Karpova, T. & McNally, J. G. Detecting protein-protein interactions with CFP-YFP FRET by acceptor photobleaching. *Curr Protoc Cytom* Chapter 12, Unit1217, <https://doi.org/10.1002/0471142956.cy1207s35> (2006).
57. Waschke, J., Drenckhahn, D., Adamson, R. H. & Curry, F. E. Role of adhesion and contraction in Rac 1-regulated endothelial barrier function *in vivo* and *in vitro*. *Am J Physiol Heart Circ Physiol* **287**, H704–711, <https://doi.org/10.1152/ajpheart.01076.2003> (2004).
58. Curry, F. R., Clark, J. F. & Adamson, R. H. Microperfusion Technique to Investigate Regulation of Microvessel Permeability in Rat Mesentery. *J Vis Exp*, <https://doi.org/10.3791/53210> (2015).
59. Carpenter, A. E. *et al.* CellProfiler: image analysis software for identifying and quantifying cell phenotypes. *Genome Biol* **7**, R100, <https://doi.org/10.1186/gb-2006-7-10-r100> (2006).
60. Team, R. C. *A language and environment for statistical computing*. R Foundation for Statistical Computing, Vienna, Austria. www.R-project.org/, 2013).

Acknowledgements

We thank J. Miyazaki for providing the Raichu-RhoA probe and S. Yonemura for contributing the α 18-catenin antibody.

Author Contributions

K.D. and W.J.: Study concept and design; K.D., R.L.T., R.M.Y., G.-P.A. and W.E.: Acquisition of data; K.D., R.L.T. and W.J.: Analysis and interpretation of data; K.D. and R.L.T.: Writing of the manuscript, preparation of figures and statistical analysis; K.D., R.L.T., W.J., and G.-P.A.: Critical revision of the manuscript for important intellectual content; All authors reviewed the manuscript.

Additional Information

Supplementary information accompanies this paper at <https://doi.org/10.1038/s41598-018-31408-3>.

Competing Interests: The authors declare no competing interests.

Publisher's note: Springer Nature remains neutral with regard to jurisdictional claims in published maps and institutional affiliations.



Open Access This article is licensed under a Creative Commons Attribution 4.0 International License, which permits use, sharing, adaptation, distribution and reproduction in any medium or format, as long as you give appropriate credit to the original author(s) and the source, provide a link to the Creative Commons license, and indicate if changes were made. The images or other third party material in this article are included in the article's Creative Commons license, unless indicated otherwise in a credit line to the material. If material is not included in the article's Creative Commons license and your intended use is not permitted by statutory regulation or exceeds the permitted use, you will need to obtain permission directly from the copyright holder. To view a copy of this license, visit <http://creativecommons.org/licenses/by/4.0/>.

© The Author(s) 2018